

Hydrogen Effects in Prestrained Transformation Induced Plasticity Steel

J.A. RONEVICH, B.C. De COOMAN, J.G. SPEER, E. De MOOR, and D.K. MATLOCK

Thermal desorption analysis (TDA) was performed on laboratory heat-treated transformation induced plasticity (TRIP) steel with 14.5 pct retained austenite (RA), ultimate tensile strength (UTS) of 880 MPa, and elongation to failure of 33 pct. Samples were tensile prestrained 5 pct at 253 K (−20 °C), 296 K (23 °C), and 375 K (102 °C) to generate different amounts of deformation-induced martensite, 10.5, 5.5, and 0.5 pct, respectively, prior to cathodically charging to a hydrogen content of 1 to 2 ppm. TDA was performed on charged samples to determine the location and strength of hydrogen trapping sites. TDA results suggest that dislocations were the main trapping sites in prestrained TRIP steel. The TDA peak intensity increased with prestrain, suggesting that the quantity of hydrogen trap sites increased with deformation. Tensile tests were performed on the four hydrogen-charged TRIP steel conditions. As confirmed with transmission electron microscope images, samples with more homogeneous dislocation distributions (*i.e.*, prestrained at 375 K (102 °C)) exhibited greater resistance to hydrogen embrittlement than samples that included a high dislocation density adjacent to the formations of strain-induced martensite (*i.e.*, samples prestrained at 253 K (−20 °C) and 296 K (23 °C)).

DOI: 10.1007/s11661-011-1075-3

© The Minerals, Metals & Materials Society and ASM International 2012

I. INTRODUCTION

HIGH-strength multiphase steels such as transformation induced plasticity (TRIP) steels, which consist of ferrite, bainite, austenite, and martensite, are being used more prevalently in the automobile industry as a means to increase strength and thereby decrease the gage of steel, enabling reduced fuel consumption. As strength levels increase, hydrogen embrittlement receives increased attention and an understanding of fundamental mechanisms involved is of interest. Hydrogen diffusivities and solubilities vary greatly between ferrite and austenite and need to be considered in multiphase microstructures such as TRIP steels.^[1–3] Specifically, the room temperature hydrogen diffusivity in ferrite is high, approximately 10^{-5} cm²/s,^[1] while the corresponding diffusivity in austenite is 10^{-12} cm²/s.^[2] As a consequence of the low solubility coupled with the high mobility in ferrite, hydrogen is expected to be distributed inhomogeneously in TRIP steel microstructures and may reside at traps, either reversible or irreversible. Hydrogen traps are defects in steel that provide lower energy sites.^[4] Reversible hydrogen traps, which may include dislocations, microvoids, or grain boundaries,

have been characterized as having binding energies less than 60 kJ/mol, whereas irreversible hydrogen traps have binding energies in excess of 60 kJ/mol.^[4] Reversible traps are weaker hydrogen traps that provide short residence times for hydrogen, but inevitably hydrogen surmounts the activation energy barrier. It has been well documented^[1,5] that diffusible hydrogen, *i.e.*, hydrogen not irreversibly trapped, is the cause for most hydrogen embrittlement failures.

Thermal desorption analysis (TDA) is a method that uses thermal activation as a means to determine the location of atomic hydrogen with respect to microstructural features. Depending on the strength of a specific type of trap, heat is required to provide the thermal energy necessary to allow hydrogen to surmount an activation energy barrier and diffuse out of the steel. Extensive research on hydrogen in iron and steel was performed,^[4,6–10] and activation energies associated with hydrogen traps, such as grain boundaries, dislocations, and microvoids, were reported to be 17.2, 26.8, and 35.2 kJ/mol, respectively. More recently, Escobar *et al.*^[11] investigated the effect of deformation on TRIP steel with 700 MPa UTS on hydrogen trapping capabilities. It was found that an increase in deformation increased the intensity of TDA peaks, where the peak intensity related to the quantity of hydrogen trapped. It was observed that the peak temperature did not change with increasing deformation, suggesting that the type of trapping site did not change with deformation.^[11] The increased peak intensity also increased with deformation. Deformation of steel generates large quantities of dislocations; furthermore, deformation of TRIP steels not only increases dislocation density but may also result in the strain-induced phase transformation of RA to martensite depending on the stability of the RA,^[12] which in

J.A. RONEVICH, Graduate Student, J.G. SPEER, Professor, E. De MOOR, Research Professor, and D.K. MATLOCK, Director, are with Advanced Steel Processing and Products Research Center, Department of Metallurgical and Materials Engineering, Colorado School of Mines, 1500 Illinois Street, Golden, CO 80401. Contact e-mail: jronevic@gmail.com B.C. De COOMAN, Professor, is with the Materials Design Laboratory, Graduate Institute of Ferrous Technology, Pohang University of Science and Technology, Pohang 790-784, South Korea.

Manuscript submitted June 20, 2011.

Article published online March 8, 2012

turn is accompanied by large quantities of dislocations generated to accommodate the shear transformation.^[13] Dislocations were reported previously^[6,7,10] as hydrogen traps.

Previous work^[5] found that hydrogen embrittlement can occur in TRIP steels at low levels of hydrogen, *i.e.*, 1 to 2 ppm. A loss of approximately 50 pct of the total elongation was observed. The sensitivity to hydrogen was attributed to the embrittlement of strain-induced martensite formed during deformation. Most of the ductility was reversed following aging for 24 hours at room temperature after charging, attributed to hydrogen evolution and the lack of extensive permanent damage induced by charging, *i.e.*, surface microcracks.^[5]

The purpose of the present study is to systematically evaluate the effects of hydrogen on as-processed and deformation-induced TRIP steel microstructures to help understand trapping mechanisms operating in TRIP steels. Samples were prestrained a fixed amount, but different volume fractions of strain-induced martensite were generated through prestraining at different temperatures. Low-temperature deformation was expected to result in significant strain-induced martensite generation, whereas high-temperature deformation would predominantly result in dislocation generation, as limited austenite fractions were expected to transform.^[12] Producing microstructures with controlled strain-induced responses allowed a comparison between the TDA of a TRIP microstructure containing predominantly new dislocations and a microstructure with both new dislocations and strain-induced martensite. Following prestraining, samples were cathodically charged with low levels of hydrogen, as developed previously,^[5] and subsequently tensile tested or analyzed by TDA.

II. EXPERIMENTAL PROCEDURE

A. Materials

A 0.19C-1.59Mn-1.63Si (wt pct), 1.2-mm-thick steel was laboratory heat treated using molten salts to produce a TRIP steel microstructure consisting of ferrite, bainite, and 14.5 pct RA.^[14] Table I shows the chemical composition of the TRIP steel. TRIP steel tensile specimens with a reduced section of 57.2 mm (2.25 in.) were prestrained 5 pct at 253 K (−20 °C), 296 K (23 °C), and 375 K (102 °C) to introduce dislocations and different amounts of strain-induced martensite. Test coupons (27.6 mm × 12.4 mm × 1.2 mm) were removed from the uniformly deformed gage length, hydrogen charged, and tested in thermal desorption analysis. A series of tensile tests was also performed for each condition in the as-charged condition. As-heat-treated samples were tested to complement prestrained samples.

Table I. Chemical Composition of TRIP Steel (Weight Percent)

C	Mn	Si	Ni	Cr	Mo	Ti	Al	N	S	P
0.19	1.59	1.63	0.02	0.03	<0.01	0.003	0.036	0.011	0.002	0.013

B. Hydrogen Charging

Steel samples were cathodically charged for 20 minutes in a 1 N H₂SO₄ + 1 mg/L As₂O₃ solution at 5 mA/cm² to produce a hydrogen concentration (as measured by a LECO* RH-404 hydrogen analyzer) of approxi-

*LECO is a trademark of LECO Corporation, St. Joseph, MI.

mately 1 to 2 ppm. Previous work^[5] verified the repeatability of this cathodic charging method. A low charging current density and short charging time resulted in no discernable damage to the surface or microstructure.

C. Thermal Desorption Analysis

Thermal desorption analysis specimens were first ground to 800 grit, cleaned with ethanol, and cathodically charged. Following charging, steel samples were removed and lightly ground with 800 grit paper to remove any buildup of oxide or arsenic residue on the surface,^[15] cleaned with ethanol, and dried. Specimens were placed into the TDA apparatus within 2 minutes after charging. The TDA system consisted of an inert gas with flow control, a temperature-controlled furnace, and a gas chromatograph for hydrogen detection. The test procedure comprised of a 15-minute purge with 99.9999 pct helium, at 10 mL/min, prior to initiation of data collection. The furnace was then turned on and samples were heated at linear heating rates. With increased temperature, hydrogen that evolved out of the steel was transported by the helium carrier gas and collected in the gas chromatograph. A VALCO INSTRUMENT** pulsed discharge detector was used

**VICI® is a registered trademark of Valco Instruments Co. Inc. and VICI AG, Houston, TX.

as the gas chromatograph. Four conditions, as-heat-treated and prestrained 5 pct at 253 K (−20 °C), 296 K (23 °C), and 375 K (102 °C), were tested at five different heating rates 373 K (100 °C), 423 K (150 °C), 473 K (200 °C), 523 K (250 °C), and 573 K (300 °C)/h with duplicates to ensure reproducibility. Peak temperatures, T_{\max} , were determined for each heating rate, and activation energies (E_a) were determined using the Kissinger analysis,^[16] as modified by Choo and Lee,^[7] to simplify the equation when linear heating rates, Φ (K/h), were imposed. Equation [1] is the final modified expression:

$$\frac{\partial \ln(\phi/T_{\max}^2)}{\partial(1/T_{\max})} = -\frac{E_a}{R} \quad [1]$$

According to Eq. [1], when data are plotted in a Φ/T_{\max}^2 vs $1/T_{\max}$ graph, a straight line is obtained, with a slope equal to $-E_a/R$, where E_a is the activation energy and R is the gas constant. There are several assumptions involved in using this simplified model to determine activation energy: (1) time for diffusion of hydrogen through the matrix is neglected and detrapping is considered the rate limiting step, (2) retrapping of hydrogen that has detrapped is neglected, and (3) hydrogen does not attach to the surface.^[6,8,17] The assumptions discussed previously can be justified in TDA by using thin samples (1.2 mm), clean surfaces, and slow heating rates.

Additionally, a specially designed set of experiments was performed on the as-heat-treated TRIP steel to further evaluate the reversibility of the hydrogen trapping sites. First, TDA tests were performed, as a function of time, on charged samples placed in the TDA system and held isothermally at room temperature; *i.e.*, the heating system was not used. Hydrogen was collected as it naturally evolved out of the steel at room temperature. A second test was performed in which a hydrogen-charged sample was aged at room temperature for 24 hours and subsequently TDA tested. The third test was performed on an uncharged steel specimen. The results were compared to charged samples heated under normal TDA testing conditions.

D. Tensile Testing

Tensile tests were performed on an electromechanical load frame on all four conditions immediately following hydrogen charging. Tensile specimens were removed

from the hydrogen-charging bath, dried, and tested within 1.5 to 2 minutes. Tests were run at a slow strain rate of $3.3 \times 10^{-4} \text{ s}^{-1}$, and a 50.8-mm (2-in.) extensometer was used in all tensile tests. Tensile samples were held at temperature (253 K (-20 °C), 296 K (23 °C), and 375 K (102 °C)) for 4 minutes in a specifically designed isothermal submersible bath,^[18] prestrained 5 pct at temperature, removed, and returned to room temperature before hydrogen charging and tensile testing to failure at room temperature.

III. RESULTS

Room temperature tensile tests on hydrogen-charged samples were performed on each of the four conditions: as-heat-treated (*i.e.*, unstrained) and 5 pct prestrained at 375 K (102 °C), 296 K (23 °C), and 253 K (-20 °C), which resulted in 14.5, 14, 9, and 4 pct remaining austenite (*i.e.*, 0, 0.5, 5.5, and 10.5 pct of strain-induced martensite), respectively, as determined by X-ray diffraction (XRD) analysis. For each condition, one stress-strain curve was selected from five tests to represent the response to hydrogen charging. The results are shown in Figure 1. Figure 1(a) compares the engineering stress-strain curve for the as-heat-treated and as-charged TRIP steel. The as-heat-treated sample exhibited continuous yielding and a total strain to failure of 33 pct. In contrast, after hydrogen charging, the low strain continuous yielding behavior was unchanged, but the total strain to failure was significantly lower, 13.5 pct, indicating the effects of hydrogen embrittlement. Figure 1(b) shows two-part stress-strain curves for

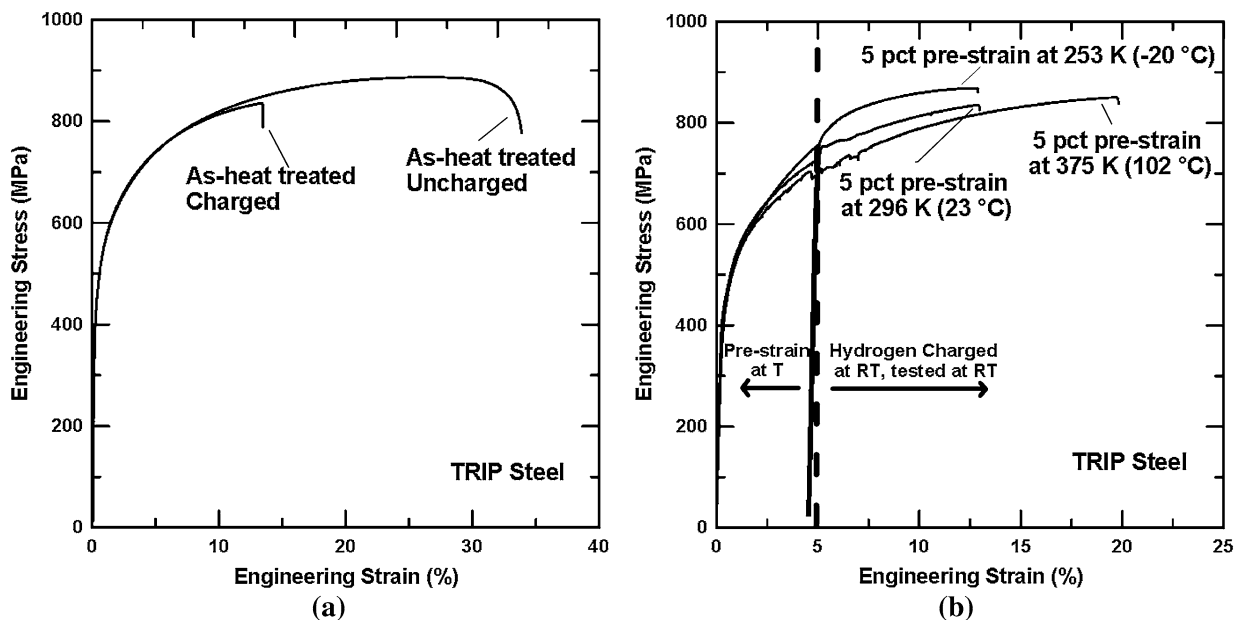


Fig. 1—Engineering stress-strain curves for TRIP steel in (a) as-heat-treated condition in uncharged and charged condition and (b) prestrained 5 pct at 253 K (-20 °C), 296 K (23 °C), and 375 K (102 °C), cathodically charged with hydrogen and tested to failure at room temperature (296 K (23 °C)). Each curve was selected from five tests and was representative of the condition to the response to hydrogen. In (b), data less than 5 pct were measured at the indicated temperature in the uncharged condition. Data collected at strains greater than 5 pct were obtained at room temperature of hydrogen-charged samples.

samples first prestrained up to 5 pct at temperatures of 253 K (−20 °C), 296 K (23 °C), and 375 K (102 °C) and then after hydrogen charging, deformed to failure at 296 K (23 °C). Immediately after reloading at 296 K (23 °C), samples prestrained at 253 K (−20 °C) exhibit a higher work hardening rate, indicative of more strain-induced martensite formation; samples prestrained at 375 K (102 °C) exhibited a lower work hardening rate and some dynamic strain aging; samples prestrained at 296 K (23 °C) exhibited intermediate work hardening behavior between the 253 K (−20 °C) and 375 K (102 °C) prestrained samples. The stress-strain response confirmed the presence of three distinct microstructures with different strain-induced martensite amounts, 10.5, 5.5, and 0.5 pct, for the samples prestrained at 253 K (−20 °C), 296 K (23 °C), and 375 K (102 °C), respectively.

Each condition was charged with the same amounts of hydrogen used in the TDA tests, *i.e.*, 1 to 2 ppm. As can be seen in Figures 1(a) and (b), hydrogen charging resulted in significant ductility loss, and all hydrogen-charged samples exhibited limited postuniform strains. The as-heat-treated and 5 pct prestrained at 253 K (−20 °C) and 296 K (23 °C) samples failed at similar strains, *i.e.*, 10 to 15 pct. However, the TRIP steel prestrained 5 pct at 375 K (102 °C) had a greater strain to failure ranging from 17 to 22 pct for the five tests at this condition.

Several comparisons can be made from Figure 1 to relate microstructural differences to tensile ductilities in samples charged with hydrogen. The RA contents were similar (14.5 and 14 pct) for the as-heat-treated (*i.e.*, unstrained) and prestrained 5 pct at 375 K (102 °C) TRIP steel microstructures, respectively. Limited strain-induced martensite (0.5 pct) formed during the 375 K (102 °C) prestrain, and the microstructure was interpreted to consist of an increased dislocation density without the formation of martensite. When hydrogen charged and tensile tested, the ductility for the 375 K (102 °C) prestrained sample (*i.e.*, 19.5 pct) was higher than the as-heat-treated sample (*i.e.*, 13.5 pct). The difference in response to hydrogen was interpreted to be due to dislocations acting as hydrogen traps and dispersing hydrogen uniformly throughout the microstructure.

A comparison of the as-heat-treated, 5 pct prestrained at 296 K (23 °C), and 5 pct prestrained at 253 K (−20 °C) values obtained by XRD showed three distinct RA contents of 14.5, 9, and 4 pct, respectively. When hydrogen charged and tensile tested, all three conditions exhibited similar ductilities of 13.5, 12.7, and 12.9 pct, respectively. The microstructure was interpreted to contain increased dislocations in ferrite adjacent to strain-induced martensite. The resulting microstructures of the four TRIP steel conditions were expected to have different dislocation distributions dependent on the formation of strain-induced martensite transformed in the initial 5 pct prestrain. Further examination of the interpreted microstructures is presented below using thermal desorption analysis and several microscopy techniques.

Examination of the microstructural constituents involved with fracture of hydrogen-charged samples

was performed using SEM imaging of longitudinal cross sections of the uniform elongated gage, *i.e.*, region away from the fracture surface. Figure 2 shows SEM images of the TRIP steel microstructures of the four conditions hydrogen charged and tested to failure: as-heat-treated (Figure 2(a)) and prestrained 5 pct at 253 K (−20 °C) (Figure 2(b)), 296 K (23 °C) (Figure 2(c)), and 375 K (102 °C) (Figure 2(d)). In all four conditions, cracks were observed to traverse martensite islands (M) and propagate perpendicular to the tensile axis and into the ferrite.^[19] As-quenched martensite was documented to be highly susceptible to hydrogen embrittlement^[20] and appears to be the susceptible phase in the present work. In contrast, for the four TRIP steel conditions uncharged, debonding or voids were observed in the martensitic regions; however, cracks or voids were limited to the martensite and did not propagate into ferrite. Similar observations can be found in the literature.^[5,21]

Hydrogen desorption *vs* temperature data for each of the four conditions for a fixed heating rate of 373 K (100 °C)/h are shown in Figure 3. Similar data were observed at other heating rates. For each TRIP steel condition, a single peak was observed at the same test temperature (T_{max}), suggesting that a single microstructural feature acted as the hydrogen trap in all four conditions. The as-heat-treated TRIP steel had the smallest intensity peak, and the three prestrained samples had similar higher intensity peaks. An increase in peak intensity with deformation was observed in previous studies.^[7] Peak intensity quantifies the number of hydrogen traps, and therefore, it can be concluded that the as-heat-treated TRIP steel contained fewer hydrogen trap sites. Each of the prestrained 5 pct samples contained different amounts of austenite and subsequently strain-induced martensite, yet appeared to have similar hydrogen trapping capabilities, *i.e.*, peak intensities.

Figure 4 shows hydrogen desorption *vs* temperature of as-heat-treated TRIP steel for five heating rates, from 373 to 573 K (100 to 300 °C)/h in 50 K (50 °C)/h increments. The peak intensities and peak temperatures increased with increasing heating rates. As heating rates are increased, the response time of hydrogen evolving out of the steel is delayed to higher temperatures,^[22] an observation that is consistent with previous work.^[23] The increase in peak intensity with heating rate corresponds to greater diffusivities at higher temperatures; *i.e.*, hydrogen released at higher temperatures will evolve more quickly than hydrogen released at lower temperatures and, in a fixed collection time, results in higher observed intensity.

The activation energies determined from this work were 28, 29, 27, and 33 kJ/mol for as-heat-treated and 5 pct prestrain at 375 K (102 °C), 296 K (23 °C), and 253 K (−20 °C) TRIP steels, respectively. For comparison, an activation energy of 26.8 kJ/mol for hydrogen trapping at dislocations was reported^[7] in commercially pure iron, as determined by TDA. Other techniques such as internal friction and gas permeation have yielded activation energies for hydrogen at dislocations in pure iron that range from 26.4 to 35.1 kJ/mol.^[10]

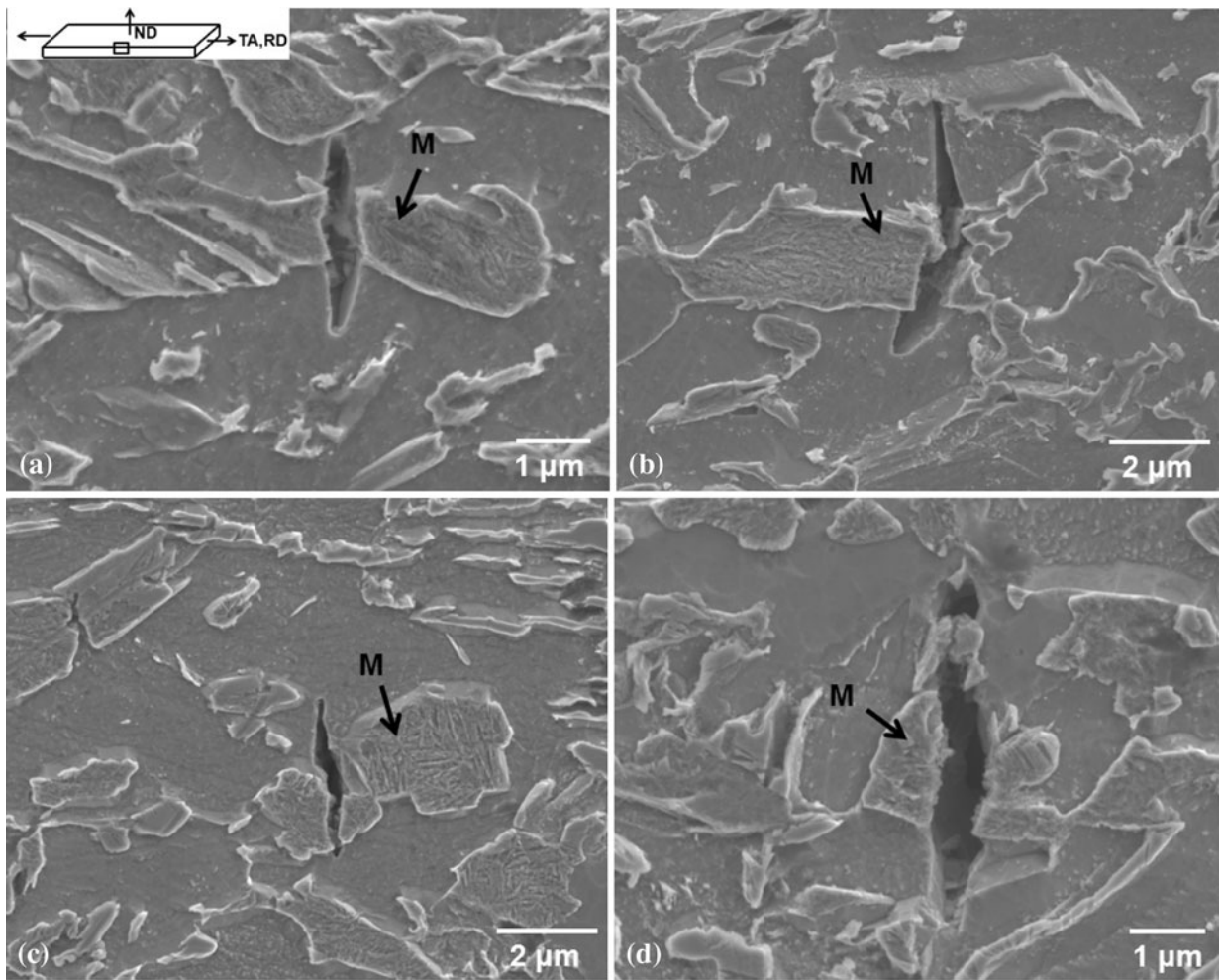


Fig. 2—TRIP steels charged with hydrogen and tensile tested to failure with the following preconditions: (a) as-heat-treated, (b) prestrained 5 pct at 253 K (−20 °C), (c) prestrained 5 pct at 296 K (23 °C), and (d) prestrained 5 pct at 375 K (102 °C). In all conditions, cracks were observed in martensite (M) and surrounding ferrite perpendicular to the tensile axis (SEM images of longitudinal cross sections, 2 pct nital etch).

Therefore, the activation energies determined in this work appear to be comparable with activation energies for hydrogen at dislocations.^[6,7,10] In contrast, previous work^[24] characterized RA as a strong hydrogen trap having a binding energy of 55 kJ/mol. Given the relatively short charging times (20 minutes) used in this study, it was not expected that austenite would have a significant role in hydrogen trapping considering the extremely low diffusivity of hydrogen in austenite.^[2]

An evaluation of the reversibility of hydrogen traps was conducted using a specially designed set of TDA tests on as-heat-treated TRIP steel. The results of these tests are summarized in Figure 5, which shows plots of hydrogen desorption vs time for four conditions. The solid line shows data for the same as-heat-treated TRIP steel from Figures 3 and 4 that was charged and placed into the TDA apparatus and heated at 373 K (100 °C)/h. The dashed line represents a sample charged and placed in the TDA apparatus, but without the application of heat. Initially, both samples exhibited decreasing parabolic behavior, indicating natural decay of hydrogen out of the steel. The dashed line mimics the trend of the solid line; however, with no supplied heat, hydrogen

continuously evolved out of the steel at a progressively slower rate. It was also observed that the as-heat-treated and hydrogen-charged sample exhibited a peak return to negligible levels of hydrogen immediately following the termination of the peak (*i.e.*, after about 80 minutes), whereas the sample held at room temperature exhibited hydrogen levels that steadily decreased up to several hours after hydrogen charging. The third and fourth lines superimposed on the plot show data for a sample that was charged and aged at room temperature for 24 hours and an uncharged sample, both heated at 373 K (100 °C)/h. The similar trend of these two curves, which exhibit negligible signals at all times, consistent with the absence of significant amounts of hydrogen, verifies that the charged hydrogen in this experiment was diffusible and reversibly trapped. Hydrogen naturally evolved out of the steel in less than 24 hours. Minimal hydrogen was initially present in the as-heat-treated sample. The results of these tests suggest that nearly all hydrogen charged into TRIP steel was diffusible or reversibly trapped hydrogen.

TDA results suggested that the dominant hydrogen trap sites in TRIP steel were dislocations. Activation

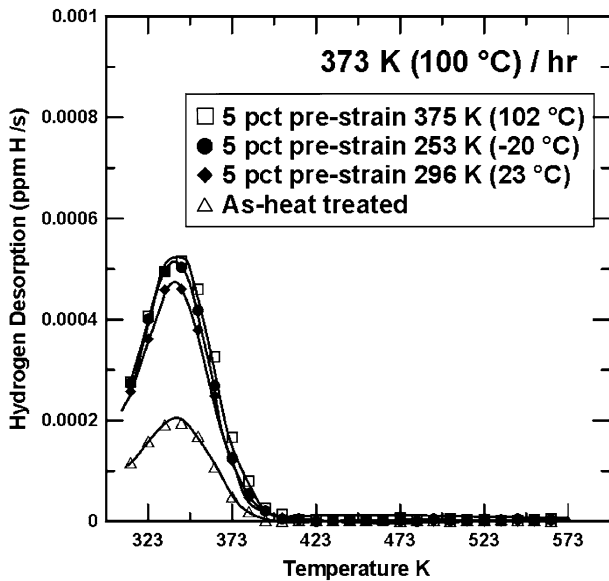


Fig. 3—Hydrogen desorption of TRIP steel in the as-heat-treated condition and after 5 pct prestrain at 253 K (-20°C), 296 K (23°C), and 375 K (102°C) for a heating rate of 373 K ($100^{\circ}\text{C}/\text{h}$).

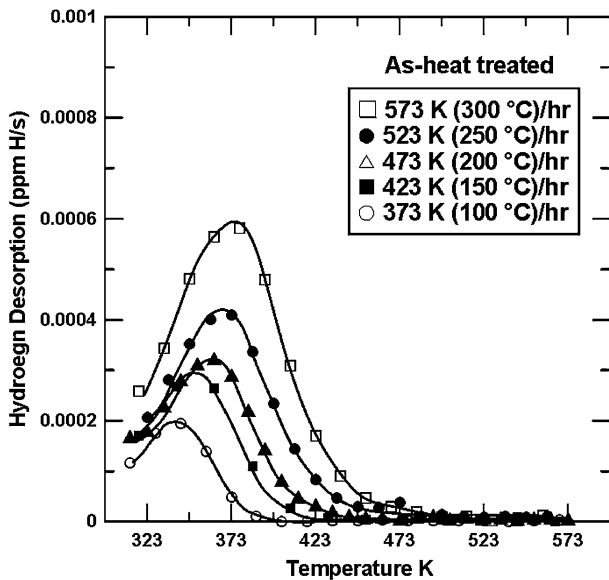


Fig. 4—Hydrogen desorption of as-heat-treated TRIP steel for five heating rates ranging from 373 K ($100^{\circ}\text{C}/\text{h}$) to 573 K ($300^{\circ}\text{C}/\text{h}$), showing the peak temperature and peak intensity increase with increasing heating rates.

energies, determined in this work, ranging from 27 to 33 kJ/mol, are similar to those found in the literature^[6,7,10] and are characteristic of reversible hydrogen traps. As shown in Figure 3, an increased quantity of trapped hydrogen was observed in the samples prestrained 5 pct. The observed higher hydrogen content was interpreted to be due to the increased dislocation density from deformation. Furthermore, dislocation distributions were expected to differ based on the prestrain temperatures due to strain-induced martensite formation, *i.e.*,

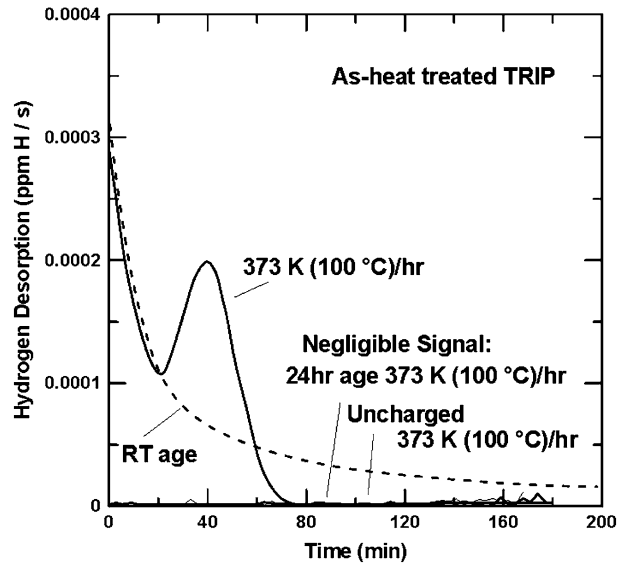


Fig. 5—Hydrogen desorption vs time for as-heat-treated TRIP steel. The sample exhibiting a desorption peak was hydrogen charged and heated at 373 K ($100^{\circ}\text{C}/\text{h}$). The dashed line represents a sample that was hydrogen charged, but without heat supplied during the hydrogen collection. The signals of the 24-hour aged sample and uncharged sample are both negligible.

more localized dislocations when martensite forms, and correspondingly more homogeneous dislocation distributions in the absence of martensite formation. To provide direct evidence of this interpretation of dislocation distributions, selected samples in the uncharged condition were examined using TEM imaging: as-heat-treated, prestrained 5 pct at 253 K (-20°C), and prestrained 5 pct at 375 K (102°C).

Figure 6 shows a bright-field TEM image of a bainitic region containing two austenite films identified by black arrows. In the undeformed condition, dislocations (identified by white arrows) were observed near the interfaces between austenite and bainitic ferrite, interpreted to be generated to accommodate bainitic transformation.^[25]

Figure 7 shows a bright-field TEM image of TRIP steel prestrained 5 pct at 253 K (-20°C). A significant difference in RA was present in this sample (4 pct RA) as compared to the as-heat-treated one (14.5 pct RA). In Figure 7, clusters of dislocations (identified by white arrows) were observed in ferrite adjacent to martensite. A distinct difference in dislocation density was observed in the ferrite adjacent to martensite compared to dislocations in the ferrite away from martensite, with higher densities in regions where martensite formed. It has been well documented^[13] that strain-induced martensite is accompanied by localized regions of dislocations to accommodate the shear transformation.

Figure 8(a) shows a bright-field TEM image of uncharged TRIP steel prestrained 5 pct at 375 K (102°C). RA levels were similar to the undeformed as-heat-treated TRIP steel; however, prestrain resulted in increased dislocation densities. As a result of limited austenite to martensite transformation during the 375 K

(102 °C) prestrain, the dislocation density in ferrite adjacent to austenite is similar to that observed for the undeformed sample in Figure 6. However, the dislocation density did increase in ferrite away from the austenite interfaces, as indicated by the white arrows. Figures 8(b) and (c) show diffraction patterns (DPs) of selected regions in Figure 8(a). The DP in Figure 8(b) is of the region in the circle on the left and was indexed as austenite and ferrite, and Figure 8(c) shows a DP

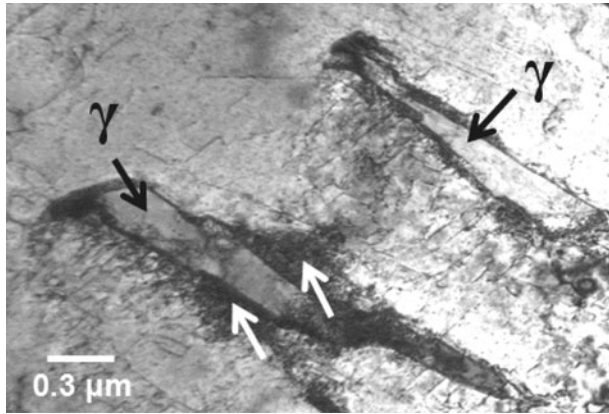


Fig. 6—Bright-field TEM image of the bainitic area in uncharged, as-heat-treated TRIP steel. Austenite is identified with a black arrow. White arrows point to areas in ferrite with increased dislocation densities.

captured from the region in the circle on the right in dislocated ferrite and confirms the structure as ferrite.

The quantity of trap sites can be evaluated in TDA by comparing intensities; however, the distribution of those traps does not affect peak intensity or temperature, as confirmed in recent work^[26] in which two ultra-high-strength steels with different cementite distributions and morphologies yielded similar thermal desorption curves when hydrogen charged. A comparison of the three TRIP steel conditions examined using TEM imaging confirmed an increased dislocation density with deformation and thus explained the increased peak intensity with deformation in Figure 3. Furthermore, dislocation distributions varied for the three select conditions. Strain-induced martensite was accompanied by localized high dislocation densities in surrounding ferrite. Pre-strain of TRIP steel at 375 K (102 °C) was observed to have a microstructure consisting of a more uniform distribution of dislocations, a structure which was anticipated to reduce hydrogen sensitivity by dispersing trap sites throughout the microstructure as opposed to localizing them at potential crack sites, *i.e.*, martensite, as determined in SEM images in Figure 2. The interpretation of traps dispersing hydrogen and resulting in reduced sensitivity was proposed previously;^[27] Pressouyre^[27] suggested that a microstructure resistant to hydrogen could be attained through a uniform distribution of trap sites to prevent or delay concentrations of hydrogen from reaching critical levels that may cause cracking.

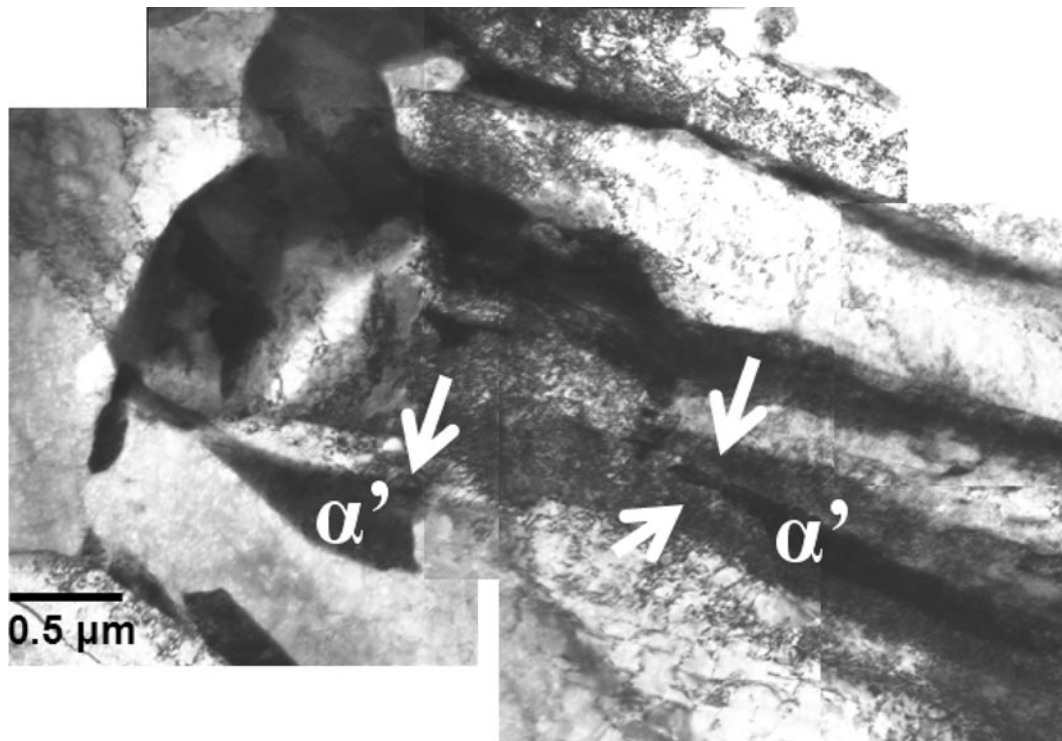


Fig. 7—Bright-field TEM image of uncharged TRIP steel prestrained 5 pct at 253 K (−20 °C). White arrows point to clusters of dislocations in ferrite near martensite interfaces. Closer examination of martensitic regions, α' , revealed twins. Ferrite, away from martensite, has lower dislocation density.

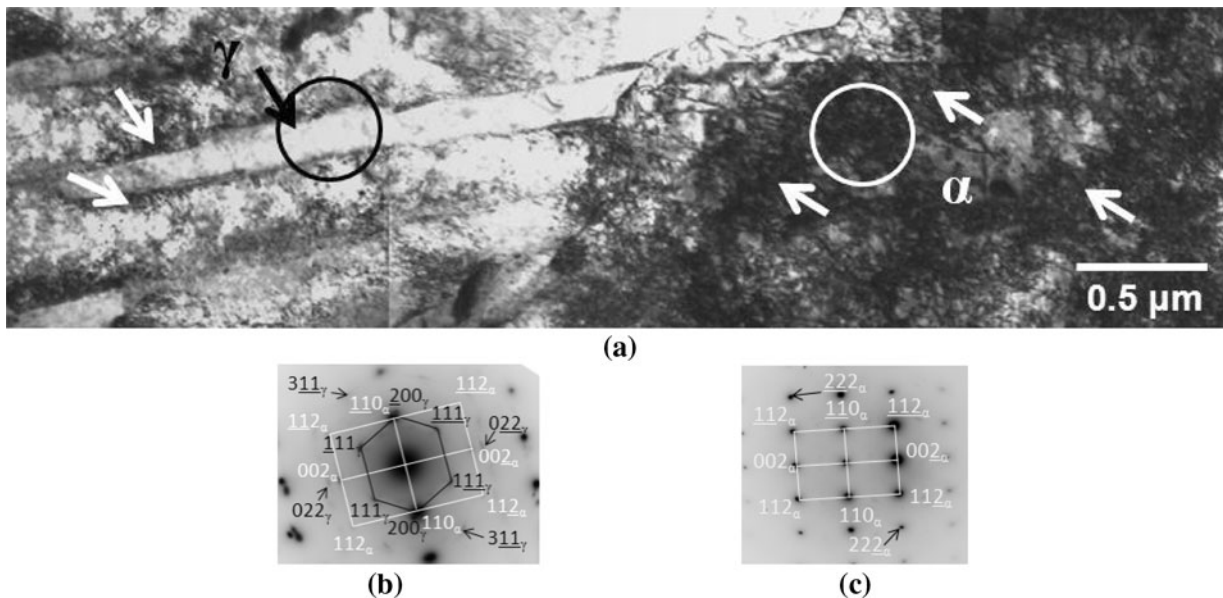


Fig. 8—(a) Bright-field TEM image of TRIP steel prestrained 5 pct at 375 K (102 °C) of an austenite film on the left with the corresponding DP shown in (b) with beam directions indexed as $[110]_z$ and $[011]_y$. The region to the right shows a highly dislocated ferrite region indexed in the white circle with the DP shown in (c) with a beam direction of $[110]_z$.

IV. CONCLUSIONS

The effects of hydrogen on deformed TRIP steels were investigated through tensile testing, thermal desorption analysis, and examination of the microstructure. The following is a list of conclusions from the present work.

1. In a TRIP steel, which initially contained 14.5 pct austenite, prestrain at 253 K (−20 °C), 296 K (23 °C), and 375 K (102 °C) produced three distinct microstructures with 10.5, 5.5, and 0.5 pct strain-induced martensite, respectively.
2. TDA results of four conditions of TRIP steel in as-heat-treated and prestrained 5 pct at 253 (−20 °C), 296 (23 °C), and 375 K (102 °C) yielded activation energies from 27 to 33 kJ/mol, values interpreted to reflect the presence of reversible traps and comparable with reported values for hydrogen trapping at dislocations.
3. TDA peak intensity increased with prestrain and indicated that the quantity of trapped hydrogen increased with deformation.
4. TRIP steel prestrained 5 pct at 375 K (102 °C) and subsequently hydrogen charged resulting in greater resistance to hydrogen when compared to all other conditions tested.
5. A specially designed set of TDA tests verified the reversibility of hydrogen trapping in TRIP steel. At room temperature, nearly all hydrogen escaped in a time period less than 24 hours, indicating that all hydrogen charged in this experiment was reversibly trapped hydrogen.
6. Fracture of martensite occurred in hydrogen-charged TRIP steel samples with crack propagation into the surrounding ferrite.
7. TEM images revealed dislocations clustered around strain-induced martensite in TRIP steel prestrained

5 pct at 253 K (−20 °C). High-temperature (375 K (102 °C)) prestrain samples showed less localized and more uniform distributions of dislocations, which is interpreted to disperse hydrogen and improve hydrogen resistance.

ACKNOWLEDGMENTS

Part of this work was performed by one of the authors (JR) at the Graduate Institute of Ferrous Technology (GIFT), Pohang Institute of Science and Technology, University in Pohang, and the authors thank GIFT for their support. This work was partially supported by the IMI Program of the National Science Foundation under Award No. DMR 0843934. The authors are also grateful for the support of the Advanced Steel Processing and Products Research Center, an industry/university cooperative research center at the Colorado School of Mines.

REFERENCES

1. J. Hirth: *Metall. Mater. Trans. A*, 1980, vol. 11A, pp. 861–90.
2. T.P. Perng and C.J. Altstetter: *Mater. Sci. Eng. A*, 1990, vol. 129, pp. 99–107.
3. A. Turnbull and R.B. Hutchings: *Mater. Sci. Eng. A*, 1994, vol. 177, pp. 161–71.
4. I. Maroef, D.L. Olson, M. Eberhart, and G.R. Edwards: *Int. Mater. Rev.*, 2001, vol. 47, pp. 191–223.
5. J.A. Ronevich, J.G. Speer, and D.K. Matlock: *SAE Int. J. Mater. Manufact.*, 2010, vol. 3, pp. 255–67.
6. W. Choo and J. Lee: *Metall. Trans. A*, 1983, vol. 14A, pp. 1299–305.
7. W. Choo and J. Lee: *Metall. Trans. A*, 1982, vol. 13A, pp. 135–40.
8. F. Wei, T. Hara, and K. Tsuzaki: *Metall. Mater. Trans. B*, 2004, vol. 35B, pp. 587–97.
9. Y. Park, I.S. Maroef, A. Landau, and D.L. Olson: *Weld. J.*, 2002, vol. 81, pp. 27–35.

10. C.M. Sturges and A.P. Miodownik: *Acta Metall.*, 1969, vol. 17, pp. 1197–1207.
11. D. Escobar, L. Duprez, K. Verbeken, and M. Verhaege: *Proc. 2008 Int. Hydrogen Conf.*, Jackson Hole, WY, 2008, ASM International, Materials Park, OH, pp. 485–92.
12. L. Samek, E. De Moor, J. Penning, and B. De Cooman: *Metall. Mater. Trans. A*, 2006, vol. 37A, pp. 109–24.
13. P.J. Jacques: *Curr. Opin. Solid State Mater. Sci.*, 2004, vol. 8, pp. 259–65.
14. A.M. Streicher, J.G. Speer, D.K. Matlock, and B.C. De Cooman: *Proc. Int. Conf. on Advanced High-Strength Sheet Steels for Automotive Applications*, J.G. Speer, ed., AIST, Warrendale, PA, 2004, pp. 51–62.
15. D. Escobar, K. Verbeken, L. Duprez, and M. Verhaege: *Proc. 2008 Int. Hydrogen Conf.*, Jackson Hole, WY, 2008, ASM International, Materials Park, OH, pp. 477–84.
16. H.E. Kissinger: *Anal. Chem.*, 1957, vol. 29, pp. 1702–06.
17. F. Wei and K. Tsuzaki: *Metall. Mater. Trans. A*, 2006, vol. 37A, pp. 331–53.
18. S.F. Peterson, M.C. Mataya, and D.K. Matlock: *JOM*, 1997, vol. 49, pp. 54–58.
19. R.G. Davies: *Scripta Metall.*, 1983, vol. 17, pp. 889–92.
20. G. Krauss: *Steels: Processing, Structure and Performance*, ASM INTERNATIONAL, Materials Park, OH, 2005.
21. T.B. Hilditch, S.B. Lee, J.G. Speer, and D.K. Matlock: *SAE Technical Publication 2003-01-0525*, SAE, Warrendale, PA, 2003.
22. A. Turnbull, R.B. Hutchings, and D.H. Ferriss: *Mater. Sci. Eng. A*, 1997, vol. 238, pp. 317–28.
23. E. Dabah, V. Lisitsyn, and D. Eliezer: *Mater. Sci. Eng. A*, 2010, vol. 527, pp. 4851–57.
24. Y. Park, I.S. Maroef, A. Landau, and D.L. Olson: *Weld. J.*, 2002, pp. 27–35.
25. H.K.D.H. Bhadeshia: *Bainite in Steels*, 2nd ed., Cambridge University Press, Cambridge, United Kingdom, 2001.
26. A. Nagao, K. Hayashi, K. Oi, and S. Mitao: *Proc. Int. Symp. on the Recent Developments in Plate Steels*, Winter Park, CO, 2011, pp. 159–67.
27. G. Pressouyre: *Metall. Trans. A*, 1979, vol. 10A, pp. 1571–73.